

ARE THE BENDING MAGNET BEAMLINES APPROPRIATE FOR PROTEIN CRYSTALLOGRAPHERS?

Pawel Grochulski

Canadian Light Source, University of Saskatchewan, 101 Perimeter Road, Saskatoon, SK S7N 0X4, Canada

Insertion device (ID) and bending magnet (BM) protein crystallography beamlines are compared for their usefulness to protein crystallographers, using as an example the Canadian Macromolecular Crystallography Facility at the Canadian Light Source. The ID beamline is concluded to be more appropriate to study small, poorly diffracting crystals with large unit cells, whereas the BM beamline is valuable for collecting diffraction data from an average protein crystal of about 100 μm in size having cell dimensions no larger than 400 \AA .

1. Introduction

Recently, small and poorly diffracting crystals with large cell dimension ($>400 \text{\AA}$) have started appearing on synchrotron beamlines. Third-generation synchrotrons have allowed for the design of more powerful third-generation beamlines. The definition of a protein crystallography third-generation beamline is somewhat arbitrary but one can specify it as a beamline where a monochromatic experiment is completed within 60 minutes or a multi-wavelength experiment is completed between 1 to 6 hours. The new third-generation beamlines can generate plenty of photons, so the exposure time is normally about 1 second; however transfer of data, readout of detector, and synchronization of the shutter still have large contributions and are estimated to be a factor of two or three with respect to the average exposure time. Other factors that substantially enhance the efficiency of a beamline are automated crystal loading and centering of the crystals.

Parameters that characterize a beamline are photon flux, emittance of source, brilliance, flux density, and photon energy resolution usually expressed in the energy bandwidth of the monochromator. The flux is defined as the number of photons per second per bandwidth (BW) and the bandwidth is usually quoted as 0.1% (*i.e.* $\Delta E/E = 10^{-3}$). For third-generation hard X-ray sources, flux levels from undulators are typically of the order of 10^{14} to 10^{15} photons/s/0.1% BW over the range from 5 to 20 keV. The emittance of source is defined as a product of source size and divergence and is given separately in horizontal and vertical plane, respectively. The emittance of source is determined by the convolution of the emittance of the electron beam circulating in the storage ring, and emittance of the photon beam for the passage of a single electron through the source path that is visible to the observer. Emittance is conserved along the beamline. Consequently, for a source with large emittance, it is not possible to get a small beam size as well as a small divergence at the focus. The brilliance is defined as photons/s/0.1%BW/mm²/mrad² and is equal to the flux divided by a product of emittance in horizontal and vertical planes. The brilliance usually ranges from 10^{18} to 10^{20} photons/s/0.1%BW/mm²/mrad². Flux levels from bending magnets (including superbends and wigglers) are typically of the order of 10^{12} to 10^{13} photons/s/0.1%BW and a brilliance range of 10^{14} to 10^{15} photons/s/0.1%BW/mm²/mrad² for the same energy range. Flux density is defined as a flux deposited on

the surface area of a crystal at the focus. The photon energy resolution is determined by the crystals of a monochromator. These crystals are most commonly fabricated from silicon due to its availability and excellent thermal properties. Although Si(111) crystals are used most frequently, beamlines located at a very brilliant sources sometimes use Si(220) crystals to further reduce the bandwidth of the monochromator. For example at energy of 10 keV the bandwidths of the Si(111) and Si(220) crystals are of 1.2×10^{-4} and 5.5×10^{-5} , respectively. The smaller bandwidth of Si(220) crystal helps to detect more precisely edges of anomalous scatterers for performing multiwavelength anomalous diffraction (MAD) experiments. In recent years diamond has become a popular alternative, due to the fact it has the highest thermal conductivity of any solid, with low absorption.

Protein crystallographers typically want a beam with a small emittance of source *i.e.* a small X-ray photon beam size to match their small crystals, as well as a small X-ray beam divergence at the crystal, since a smaller divergence of the beam at the sample will produce a smaller diffraction spot on the detector. With adequate X-ray optics, a small beam size at the crystal position can be accomplished either from a bending magnet or undulator. However, obtaining a small divergence of beam at the same time requires the source to have a large brilliance. In the case of extremely small crystals, of the order of 5 - 20 μm , a micro-focusing undulator beamline is most appropriate. Building a micro-focusing beamline requires a synchrotron facility with a low electron emittance ($< 5 \text{ nm} \times \text{rad}$). The ID13 beamline at European Synchrotron Radiation Facility is an example of such a beamline.

In general, the decision as to which beamline is appropriate for a given diffraction experiment can be made on the basis of the following inequality, which relates the crystal to detector distance (L), to the synchrotron radiation wavelength (λ), maximum cell dimension (a), size of the crystal (s) and beam divergence at the sample (δ).

$$L > s/((\lambda/a) - \delta) \quad (1)$$

It was derived from the assumption that the spot spacing on a detector must be bigger than the spot sizes in order to resolve them [1]. As the detector moves towards the sample the angle ($2\theta_{\text{max}}$) captured by the detector increases allowing higher resolution reflections to be captured at the edge of the detector ($D/2$), where D is the size of a detector. Resolution is defined as the d-spacing that according to Bragg's

law corresponds to the angle at the edge of the detector.

$$2d_{min} \sin \Theta_{max} = n\lambda \quad (2)$$

The resolution as a function of the wavelength and the crystal to detector distance are given in the following equations:

$$d_{min} = \lambda / (2(\sin(\arctan(D/2L)))) \quad (3)$$

$$L = (D/2) / (\tan(2\arcsin(\lambda/2d_{min}))) \quad (4)$$

From the above inequality, smaller crystals allow for a smaller detector distance, which increases the resolution. The distance can be reduced further when the beam divergence is small. Therefore an insertion device beamline is clearly more advantageous for collecting data from small crystals with large cell dimensions. The wavelength of synchrotron radiation is also a factor; therefore using shorter wavelengths will be beneficial for getting higher resolution at the edge of the detector at a given crystal to detector distance. It should be mentioned that the pixel size of the Xray detector needs to be considered as well. The typical pixel size of a modern CCD X-ray detector is at the order of 50-70 μm and is sufficient for current requirements of protein crystallographers.

2. Radiation Damage

High brilliance synchrotron beamlines are one of the most powerful tools for modern protein crystallography. However, their usage often results in serious problems due to radiation damage of crystals even at liquid nitrogen temperatures. In 1990 Henderson [2] proposed a maximum dose limit of 2×10^7 Gy, which reduced to half the diffraction intensity of a protein crystal in electron microscopy. Since then the limit has been verified experimentally at various protein crystallography beamlines. This limit corresponds to 1.6×10^{16} photons/ mm^2 deposited on the crystal and it was shown for lysozyme crystals [3] that radiation damage is not dependent on incident photon energy between 6.5 keV and 33 keV. Therefore a flux density of 10^{14} photons/s/ mm^2 deposited on an average protein crystal of 100 μm x 100 μm will destroy it after several minutes of exposure. On micro-focusing beamlines the flux density has to be monitored very closely - for example using RADDPOSE [4] and BEST [5] - and a careful strategy of data collection has to be performed in order to collect a full data set from one protein crystal. It should be mentioned, that in some cases specific radiation damage can be an opportunity for phasing molecular structures [6].

In this era of structural genomics, small crystals (~ 20 μm) are frequently obtained using crystallization robots. Those small crystals usually have fewer imperfections, however the standard kinematics theory of diffraction assumes that the lattice is a quasi-infinite array of unit cells,

and the sharp rocking curve widths of the Bragg reflection occur because of massive scattering overlap from the individual unit cells. These assumptions do not hold when the number of unit cells along one dimension of the crystal becomes smaller than about 1000, so crystals with fewer than 1000^3 unit cells will display broadened reflection profiles. For example, for a cell dimension of 100 \AA , the limit on the crystal size would be 10 μm . Crystals smaller than that would likely have their rocking curves broadened and diffract poorly [7].

3. Introduction to the Canadian Light Source

The Canadian Light Source (CLS), located at the University of Saskatchewan, is a 2.9 GeV third-generation synchrotron facility. The CLS consists of a 250 MeV electron Linac, a booster to bring the electron beam energy to 2.9 GeV, and the storage ring, which is designed to operate at a current of up to 500 mA. The ring currently operates with a current of 250 mA - in order to bring it to 500 mA a second superconducting RF cavity has to be installed in the storage ring. The ring's specifications are shown in Table 1 and source electron beam sizes and divergences for BM and ID are shown in Table 2. Depending on energy, the horizontal and vertical emittance of the source are bigger than electron beam emittances [8], however from a practical point of view the electron beam sizes in the X-ray regime can be used as guidelines for initial beamline design. The ratio of the emittance in the vertical and horizontal directions is known as coupling. For example if coupling is chosen to be 1% it means that the horizontal emittance is of 100 times larger than in the vertical emittance.

Table 1. CLS ring specifications.

	Nominal	Long-term goals
Energy (GeV)	2.9	2.9
Current (mA)	250	500
Time structure	multi-bunch	multi-/single-bunch
Horizontal Emittance ($\text{nm} \times \text{rad}$)	<20	18.1
Energy Spread (%)	0.11	0.11
Lifetime (h)	> 6	> 10 (or Top-up)
x-y Coupling (minimum) (%)	<1	< 0.2
ν	5675.3	5675.3
λ_c (\AA)	1.6378	1.6378
E_c (keV)	7.572	7.572
Circumference (m)	170.88	170.88
Dipole Field (T)	1.354	1.354

All of the initial X-ray beamlines built during the first phase of development of the CLS were beamlines based on insertion devices and their brilliances are shown in Figure 1. With the exception of the superconducting wiggler, all insertion devices were designed, assembled and shimmed at the CLS.

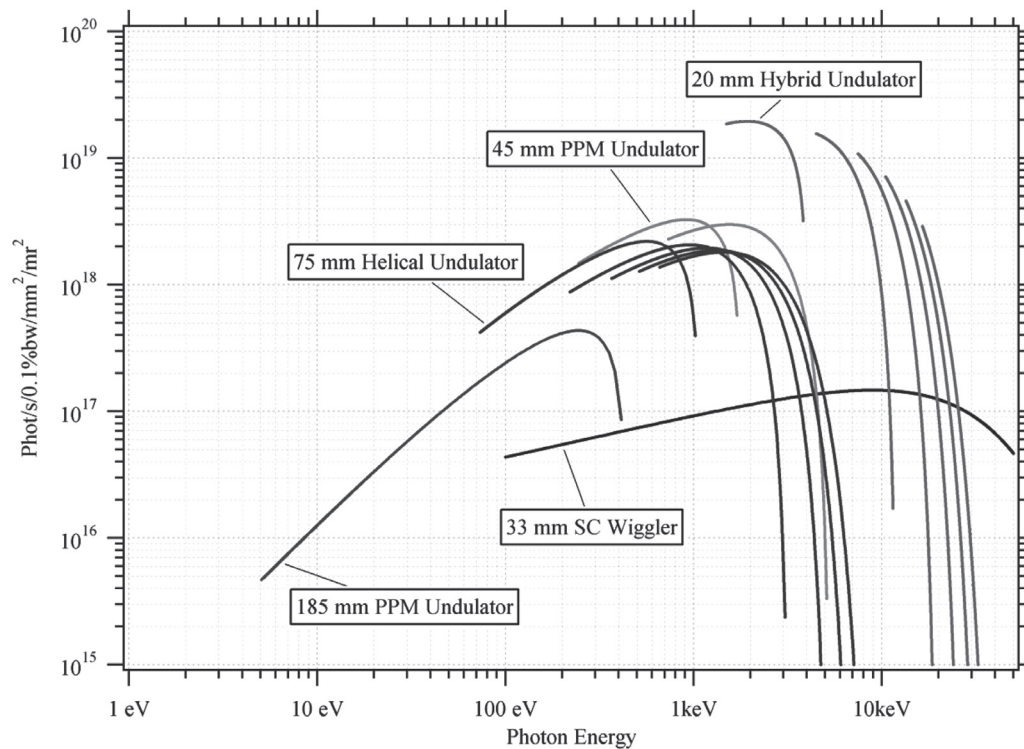


Figure 1. Brilliance at the CLS - tuning curves for insertion devices currently installed in the storage ring. The number at the beginning of the label describes the length of the period of the device. PPM stands for pure permanent magnet and SC stands for a superconducting device.

Table 2. Source electron beam sizes and divergences at dipole magnets ($T_{unex}=10.22$, $T_{uney}=4.32$, dispersion in straights=0.25, 0.2% coupling).

Beamline source	Horizontal		Vertical	
	σ_x [mm] Size	σ_x [mrad] Divergence	σ_y [mm] Size	σ_y [mrad] Divergence
BM1	0.120	0.181	0.030	0.005
Straight/ID	0.438	0.041	0.008	0.003

4. The Canadian Macromolecular Crystallography Facility

The Canadian Macromolecular Crystallography Facility was formed by Canadian protein crystallographers and is envisioned to eventually consist of three beamlines - two insertion devices beamlines and one bending magnet beamline [9, 10]. The first insertion device beamline (08ID1) was intended to be highly efficient and flexible, capable of satisfying the requirements of the most challenging and diverse crystallographic experiments, i.e. physically small crystals with large unit cell dimensions. The bending magnet 08B1 beamline that is currently being built is dedicated to high-throughput data collection and will be capable of remote access. The third, an undulator based 08ID-2 beamline, is envisioned to have micro-focusing capabilities with some restrictions in energy range (Figure 2).

5. Insertion Device Beamline

The CMCF 08ID-1 beamline has been built and now is being commissioned [10]. The beamline is illuminated by a

small-gap in-vacuum hybrid undulator (SGU), located in the upstream half of the straight section, and chicaned in-board by 0.75 mrad. The downstream half of this section is reserved for the 08ID-2 beamline's SGU. The insertion device contains 80 magnetic periods with a period length of 20 mm. Magnets are made of $\text{Sm}_2\text{Co}_{17}$ and poles are made of vanadium permendur. A flux spectrum at a 5.8 mm gap is shown in Figure 3. To cover the 6.5 keV to 18 keV energy range harmonics from 3 to 9 need to be used.

The overall design of the beamline consists of white beam slits (WBS), a double crystal monochromator (DCM) equipped with an indirectly cryo-cooled first crystal and a sagittally-focusing second crystal, followed by a vertically focussing mirror (VFM). An innovative and very robust endstation, including the MarMosaic225 CCD X-ray detector completes the beamline. The beamline is equipped with a Röntek Spectrometer System (XFLASH 101A), capable of carrying out X-ray spectroscopy for multi-wavelength anomalous diffraction (MAD) and X-ray absorption near edge structure (XANES) on the same crystal, and X-ray fluorescence (XRF) for the detection of metal atoms in protein derivative crystals.

The SHADOW [11] ray-tracing results are shown in Figure 4. Calculations were done using the following parameters - a small-gap in-vacuum undulator (SGU), $k = 1.63$, $E = 12.0$ keV, 7th harmonic. Energy resolution from SHADOW, $\Delta E = 1.6$ eV so $\Delta E/E = 1.6$ [eV]/12000 [eV] = 1.33×10^{-4} and flux in [ph/s/0.1%BW] has to be multiplied by 0.133 to get the flux in [ph/s] (Table 3).

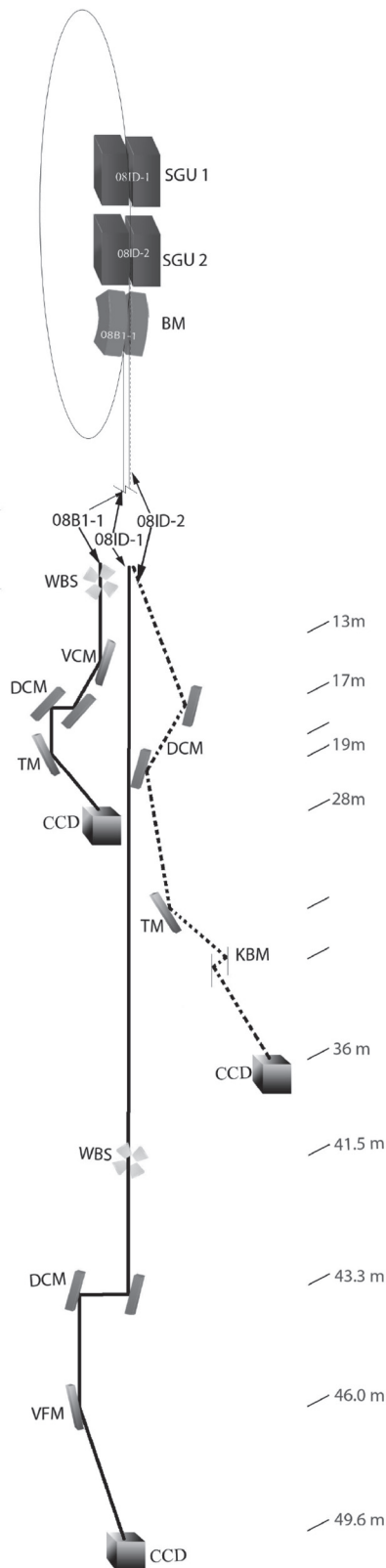


Figure 2. Layout of the Canadian Macromolecular Crystallography Facility at the Canadian Light Source. The 08ID-2 beamline (dotted lines) is shown as a conceptual design. WBS - white beam slits, VCM - vertically collimating mirror, DCM - double crystal monochromator, TM toroidal mirror, KBM - Kirkpatrick and Baez mirror system, VFM - vertically focusing mirror. CCD - end-station.

Table 3. Flux on the sample at 12.0 keV for the 08ID-1 beamline.

	Cal. Flux [phs/0.1% BW]	Undulator efficiency*	Mirror reflectivity (Pd)	Mono crystal reflectivity	Monochromatic flux on sample [ph/s]
Loss factor	1.0	0.90	0.93	0.80	0.133
	7.0×10^{13}	6.3×10^{13}	5.9×10^{13}	4.7×10^{13}	6.2×10^{12}

6. Bending Magnet Beamline

The bending magnet fan has an opening of 1 mrad (H) by 0.25 mrad (V) (Figure 4). Since the vertical opening of the bending magnet synchrotron light is larger than for insertion device, the first element of the beamline has to be a vertically focusing mirror (VFM) (Figure 2). It is followed by a double crystal monochromator with a water cooled first crystal and a toroidal mirror (TM). The location of the toroidal mirror was selected to have a horizontal demagnification of 2, since it is known that this geometry produces an image with the smallest aberrations [13]. Compared to the ID beamline, the photon energy was enlarged to include 4 keV, to enhance the anomalous and dispersive signal from sulfur atoms naturally present in proteins (at 4 keV, $f''(\text{S}) = 1.9 \text{ e}$). It should be pointed out that the CLS bending magnet source is naturally suited for a low energy range, since more flux is created at 4 keV (Figure 5). Although the Be window, that is needed to terminate the beamline, will transmit only $\sim 60\%$ of the 4 keV photons, it will still produce a very reasonable flux at the sample crystal.

The SHADOW ray-tracing results are shown in Figure 6. Calculations were done using the following parameters - energy resolution from SHADOW, $\Delta E = 1.5 \text{ eV}$ so $\Delta E/E = 1.5 \text{ [eV]}/12000 \text{ [eV]} = 1.25 \times 10^{-4}$ and flux in [ph/s/0.1%BW] has to be multiplied by 0.125 to get flux in [ph/s] (Table 4).

Table 4. Flux on the sample @ 12 keV for BM beamline taking into account losses at the optical elements.

	Flux [ph/s/0.1% BW]	Mirror reflectivity (Rh)	DCM crystals reflectivity	Monochromatic flux on the sample [ph/s]
Loss factor	1	0.93×0.93	0.80	0.125
	5.6×10^{12}	4.8×10^{12}	3.8×10^{12}	4.8×10^{11}

7. Comparison of the ID and BM beamlines

A comparison of the ID beamline with the BM is given in Table 5. In the ID beamline case, the vertical size of the focused beam at the sample was optimized for $50 \mu\text{m}$ as compared to the legend in Figure 4 due to gravity sag and other imperfections. The flux densities were calculated by dividing the flux by the focal size. The beam divergence at the sample was calculated with SHADOW. Due to the relatively large horizontal emittance of the CLS ring, the X-ray optics of the ID beamline needed dynamic sagittal focusing of the second monochromator crystal, which

requires the bending radius to be changed with a change of energy of the monochromator, making operation of the beamline more complicated. The toroidal mirror (TM) of the BM beamline provides for a static horizontal focusing,

not requiring adjustment with energy change, but allowing much simpler optimization of the beamline after the energy change.

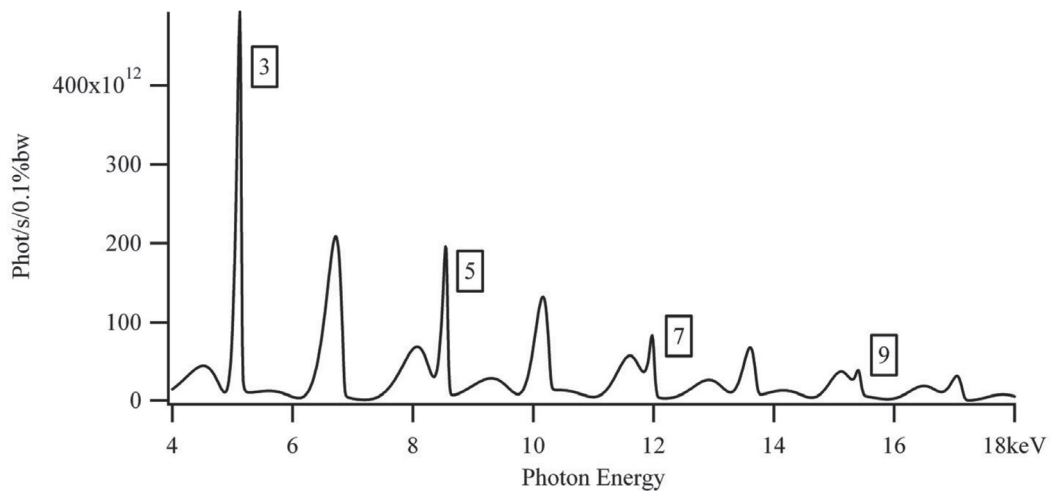


Figure 3. Flux spectrum of the CLS SGU at gap of 5.8 mm ($k = 1.63$) (SRW [12]). The first and second harmonics are not included. Even harmonics (not labeled) can be seen between the odd order harmonics.

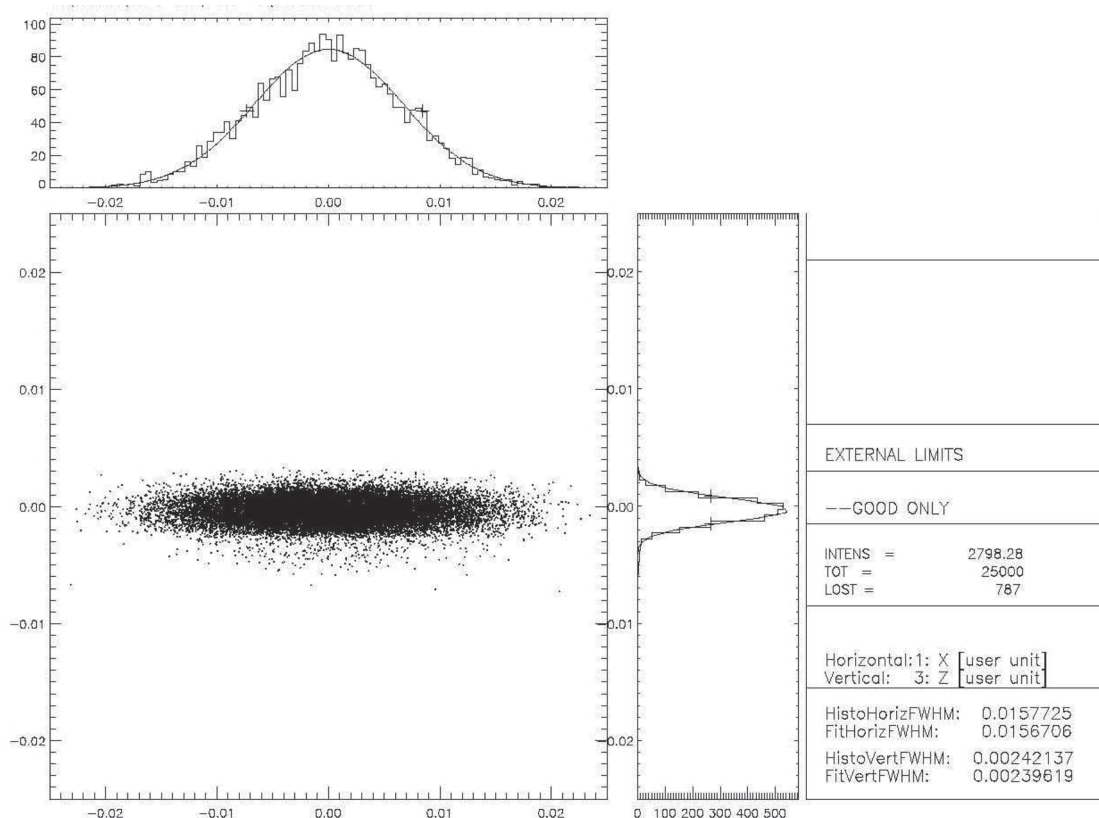


Figure 4. SHADOW ray-tracing results for the 08ID-1 beamline (focus on the sample is $160 \mu\text{m} \times 25 \mu\text{m}$ (FWHM), including tangential and sagittal rms slope errors of $1 \mu\text{rad}$ and $25 \mu\text{rad}$, respectively).

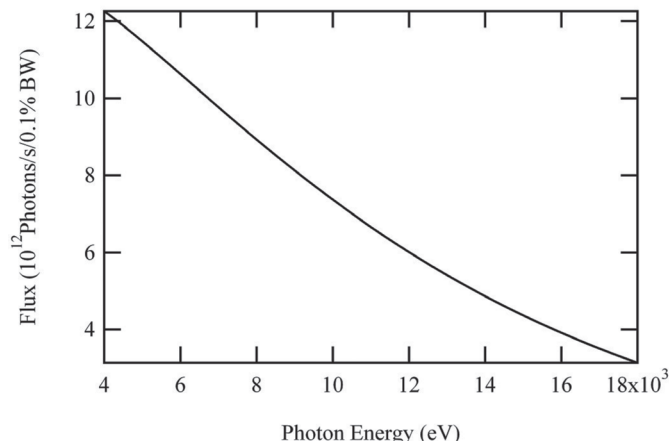


Figure 5. Flux spectrum of the CLS BM through a 1 mrad (H) \times 0.25 mrad (V) aperture (SRCalc [14]).

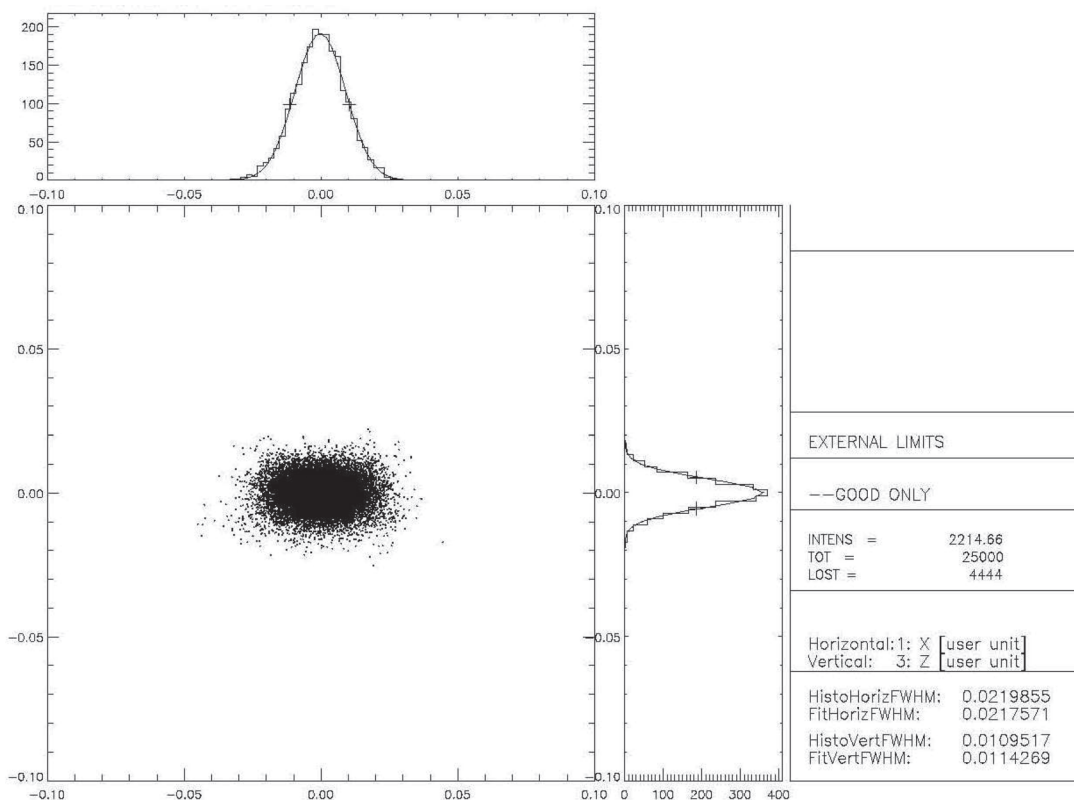


Figure 6. SHADOW ray-tracing results for the 08B1 beamline. Focus on the sample is 220 μm (H) \times 115 μm (V) (FWHM), including tangential and sagittal rms slope errors of 2 μrad and 25 μrad , respectively.

8. Discussion

ID and BM beamlines are compared with respect to their usefulness to protein crystallographers. The comparison is done using the ID and BM beamlines of the Canadian Macromolecular Crystallography Facility at the Canadian Light Source. Table 5 contains compared side by side the most important parameters of both beamlines. The flux density and the divergence at the sample are the most profound differences. The ID beamline is designed mostly to collect data from small ($> 20 \mu\text{m}$) protein crystals with large cell dimensions ($\sim 1000 \text{ \AA}$) whereas the BM beamline is very ap-

propriate to perform diffraction experiments from average crystals with cell dimensions less than 400 \AA .

Maturation of the insertion devices technology enables construction of ID protein crystallography beamlines on $\sim 3 \text{ GeV}$ rings, however the SGU needs to be in-vacuum. To be able to cover the appropriate energy range, higher harmonics have to be used which imposes demanding conditions on the quality of the rms phase errors of the SGU and complicates design of the monochromator since the power density that is deposited on the first crystal of the monochromator has to be dissipated by a cryogenic

Table 5. Comparison of the ID beamline line with the BM beamline.

	08ID-1	08B1
Spectral range (keV)	6.5 – 18.0	4.0 – 18.0
Energy bandwidth ($\Delta E/E$) for Si(111) at 12 keV	1.33×10^{-4}	1.25×10^{-4}
Flux on the sample @ 1 2 keV [photons/s]	$>10^{12}$	$>10^{11}$
Focal size (HxV) @ 12 keV [$\mu\text{m} \times \mu\text{m}$] (FWHM)	167 [H] \times 50 [V]	233 [H] \times 114 [V]
Flux density [ph/s/mm ²] @ 12 keV	$> 10^{14}$	$>10^{12}$
Beam divergence at the sample [mradxmrad] @ 12 keV (FWHM)	0.7 [H] \times 0.2 [V]	1.7 [H] \times 0.3 [V]

system. On the other hand, the first crystal of the monochromator of the BM beamline can be cooled by water.

The simplified X-ray optics of the BM beamline allows this beamline to be fully automated, so the lower flux can be compensated for, making this beamline a good candidate for remote access and mail-in crystallography.

Radiation damage is a real problem at third-generation protein crystallography beamlines. It is more severe at ID beamlines, but it must also be considered at BM beamlines as well. Knowledge of the size of the crystal and flux generated by the beamline allows calculation of the maximum allowed dose for a crystal. That in turn puts stronger emphasis on the strategy of data collection to enable a full data set to be collected from one crystal.

One might ask why protein crystallographers need so much flux density at their crystals? For a very small crystal with large cell dimensions, the beam needs to either be focused at the CCD detector or to be defocused (making it almost parallel), in order to avoid overlapping of spots on the detector. Slits can then be used to tailor the beam size to the size of the crystal. This will reduce the total flux and the flux density on the sample to values much smaller than the ones presented in Table 5. Therefore the more flux a beamline can produce the more flexibility crystallographers have for collecting data fast and registering diffraction spots from very small crystals.

Acknowledgments: The author would like to thank Dr. Brian Yates for his help with SHADOW calculations, Dr. Michel Fodje

for suggestions and careful reading of the manuscript, Dr. Les Dallin for his help with machine parameters, and Dr. Ingvar Blomqvist who designed and built insertion devices at the CLS.

References

- [1] R. Sweet, private communication, <http://www.px.nsls.bnl.gov/>.
- [2] R. Henderson, „Cryo-protection of protein crystals against radiation damage in electron and X-ray diffraction”, *Proc. R. Soc. Lond. B* **241** (1990) 6-8.
- [3] N. Shimizu, K. Hirata, K. Hasegawa, G. Ueno, M. Yamamoto, „Dose dependence of radiation damage for protein crystals studied at various X-ray energies”, *J. Synchrotr. Radiat.* **14** (2007) 4-10.
- [4] J.W. Murray, E.F. Garman, R.B.G. Ravelli, „X-ray absorption by macromolecular crystals: the effects of wavelength and crystal composition on absorbed dose”, *J. Appl. Crystallogr.* **37** (2004) 513-522.
- [5] G.P. Bourenkov, A.N. Popov „A quantitative approach to data-collection strategies”, *Acta Crystallogr. D* **62** (2006) 58-64.
- [6] S. Banumathi, P.H. Zwart, U.A. Ramagopal, M. Dauter, Z. Dauter, „Structural effects of radiation damage and its potential for phasing”, *Acta Cryst. D* **60** (2004) 1085-1093.
- [7] A.J. Howard, in: *Macromolecular Crystallography at Third-generation Synchrotron Sources. Third Generation Hard X-ray Synchrotron Radiation Sources: Source Properties, Optics, and Experimental Techniques*, D.M. Mills (Ed.), (John Wiley & Sons Ltd., New York, 2002).
- [8] J. Als-Nielsen, D. McMorrow, *Elements of Modern X-ray Physics* (John Wiley & Sons Ltd., New York, 2001)
- [9] P. Grochulski, I. Blomqvist, B. Yates, E. Hallin, L. Delbaere, „Design of the 08ID-1 protein crystallography beamline at the Canadian Light Source”, *Acta Phys. Polon. A* **101** (5) (2002) 589-594.
- [10] P. Grochulski, I. Blomqvist, L. Delbaere, „Status of the Canadian Macromolecular Crystallography Facility: Design and Commissioning of the 08ID-1 Beamline at the Canadian Light Source”, *PiC* **62** (5) (2006) 301-304.
- [11] C. Welnak, G.J. Chen, F. Cerrina, „SHADOW: a synchrotron radiation X-ray optics simulation tool”, *Nucl. Instrum. Meth. A* **347** (1994) 344-347.
- [12] O. Chubar, P. Elleaume, SRW, v. 3.7. Copyright ESRF 1997-2000.
- [13] A.A. MacDowell, R.S. Celestre, M. Howells, W. McKinney, J. Krupnick, D. Cambie, E.E. Domning, R.M. Duarte, N. Kelez, D.W. Plate, C.W. Cork, T.N. Earnest, J. Dickert, G. Meigs, C. Ralston, J.M. Holton, T. Alber, J.M. Berger, D.A. Agard, H.A. Padmore, „Suite of three protein crystallography beamlines with single superconducting bend magnet as the source”, *J. Synchrotr. Radiat.* **11** (2004) 447-455.
- [14] R. Reininger, SRCalc v. 1.2.1, 2001, <http://www.sas-rr.com/>.